Structure and Properties of Phase Change Materials Based on HDPE, Soft Fischer-Tropsch Paraffin Wax, and Wood Flour

M. E. Mngomezulu,[1] A. S. Luyt,[2] I. Krupa[3]

[1]*Department of Chemistry, University of the Free State (Qwaqwa Campus), Phuthaditjhaba 9866, South Africa*
[2]*Natural and Agricultural Sciences, University of the Free State (Qwaqwa Campus), Phuthaditjhaba 9866, South Africa*
[3]*Polymer Institute, Slovak Academy of Sciences, Bratislava 842 36, Slovak Republic*

Received 18 February 2010; accepted 25 March 2010
DOI 10.1002/app.32521
Published online 3 June 2010 in Wiley InterScience (www.interscience.wiley.com).

ABSTRACT: Phase-change materials based on high density polyethylene (HDPE), soft Fischer-Tropsch paraffin wax (M3), and alkali-treated wood flour (WF) were investigated. The blend and composite samples were prepared by melt mixing using a Brabender Plastograph, followed by melt pressing. They were characterized in terms of their morphology, as well as thermal, mechanical, thermomechanical, and water absorption properties. Although SEM micrographs showed some evidence of intimate contact between the WF particles and the HDPE matrix as a result of alkali treatment, poor filler dispersion, and interfacial adhesion were also observed. Partial immiscibility of the HDPE and the M3 wax was noticed, with the WF particles covered by wax. There was plasticization of the HDPE matrix by the wax, as well as partial cocrystallization, inhomogeneity and uneven wax dispersion in the polymer matrix. The HDPE/WF/M3 wax composites were more homogeneous than the blends. The presence of wax reduced the thermal stability of the blends and composites. Both the presence of M3 wax and WF influenced the viscoelastic behavior of HDPE. The HDPE/M3 wax blends showed an increase in the interfacial amorphous content as the wax content increases, which resulted in the appearance of a β-relaxation peak. The presence of M3 wax in HDPE reduced the mechanical properties of the blends. For the composites these properties varied with WF content. An increase in wax content resulted to a decrease in water uptake by the composites, probably because the wax covered the WF particles and penetrated the pores in these particles. J Appl Polym Sci 118: 1541–1551, 2010

Key words: HDPE; soft paraffin wax; wood flour; blends; composites; morphology; physical properties

INTRODUCTION

The development of phase change materials (PCMs) has evolved for the past 4 or 5 decades. The research in this field has led to recent formulations of form-stable or shape-stabilized PCMs. These substances have the ability to absorb, store, and release large quantities of energy. They achieve this by means of melting and solidifying at certain temperatures. For their use in thermal energy storage systems, PCMs should be economically viable and possess desirable characteristics such as thermo-physical, chemical, and kinetic properties.[1–6,7] They are used as thermal energy storage media in areas of space craft, refrigeration and conditioning systems, conservation processes, solar energy systems, energy recovery, as well as heating and cooling of buildings. To suit a given application, PCMs are selected on the basis of their melting temperature.[6,8,9]

They are classified into organic and inorganic compounds, as well as eutectic mixtures of these compounds, that all give different phase transition temperatures. Amongst these three classes, organic compounds, generally, are the most broadly studied, and paraffin waxes in particular are of recent research interest due to their promising properties as phase change materials.[2,3,5,7,8,10] They have a high latent heat of fusion, negligible super cooling, low vapor pressure in the molten state, they are chemically inert, have chemical stability, are self-nucleating, commercially available, ecologically harmless, readily available, and inexpensive. Their specific heat capacity is about 2.1 J g^{-1} K^{-1}, and their enthalpy lies between 180 and 230 kJ kg^{-1}. The combination of these two values results in an excellent energy storage density.[1,2,8,9]

As conventional solid–liquid phase change materials, it is inconvenient to use paraffin waxes directly as PCMs. Mixing of the phase change materials in polymers is the most convenient method to prevent leaking of molten material during a phase change. One of the best way to achieve this is to blend polyolefins with paraffin waxes.[1–3,9-12] There were a few studies on the blending of polyolefins with paraffin

Correspondence to: A. S. Luyt (LuytAS@qwa.ufs.ac.za).

waxes, especially on their morphology, thermal and thermo-mechanical properties,[1,2,9,13–17] but not much has been done on the determination or improvement of their mechanical properties.

Sari,[9] Inaba and Tu,[16] and Hong and Xin-shi[17] investigated HDPE/paraffin form-stable PCM blends. They reported that the paraffin was well dispersed into the net-like crystal structure of HDPE, which prevented any leakage of molten paraffin during the heat storage process. It was also found that HDPE and paraffin interacted physically rather than chemically. Krupa et al.[1,2] blended isotactic polypropylene (PP) and low density polyethylene (LDPE) with a soft petroleum wax (Wax S), and a hard oxidized Fischer-Tropsch paraffin wax (Wax FT). From both studies, it was found that these PCM blends were immiscible and that the paraffin waxes reduced the thermal stability of the polyolefins. It was also shown that an increase in wax content in the LDPE/soft petroleum wax blends led to a decrease in the ultimate strength and elongation properties. For a PCM blended with a polyolefin to be effective, the wax:polymer ratio should be high, but this generally decreases the mechanical properties and thermal stabilities of the polyolefins.[11,18] This problem could be solved with the inclusion of natural filler into the PCM blend which may improve the strength and thermal stability of the PCM.[19] The natural filler's inherent drawbacks such as poor interfacial adhesion between the hydrophobic polymer and the hydrophilic wood filler, and high water uptake could be overcome through chemical modification of a filler.[20–22] In this study, we investigated whether the incorporation of natural filler (wood flour) in PCM blends could improve their mechanical properties and thermal stability. The blends and composites were characterized in terms of their morphology, as well as thermal, mechanical, thermo-mechanical, and water absorption properties.

EXPERIMENTAL

HDPE was supplied in pellet form by DOW Chemicals, South Africa. It has an MFI of 8 g/10 min (ASTM D-1238), a molecular weight of 168,000 g mol^{-1}, a melting point of 130°C, and a density of 0.954 g cm^{-3}. Soft paraffin wax (M3 wax) was supplied in powder form by Sasol Wax. It is a paraffin wax consisting of approximately 99% of straight short chain hydrocarbons and few branched chains, and is primarily used in the manufacturing of candles. It has an average molar mass of 440 g mol^{-1} and a carbon distribution of C15–C78. It has a density of 0.90 g cm^{-3} at 25°C and a melting point range of 40–60°C. Pine wood flour was a cream-white powder supplied by Taurus furniture manufacturers, Phuthaditjhaba, South Africa. This wood flour was sieved with a laboratory sieve and it had a range of particle sizes smaller than 150 μm. Sodium hydroxide was supplied in pellet form by Associated Chemical Enterprises (ACE) (Pty), South Africa. It was a chemically pure (CP) grade with an assay of 97%. A chemically pure (CP) grade glacial acetic acid with an assay of 99.8% was supplied by Laboratory Consumables & Chemical Supplies, Durban, South Africa.

TABLE I
Sample Ratios Used for the Preparation of the Different Blends and Composites

Sample	HDPE (w/w)	M3 wax (w/w)	WF (w/w)
1	100	0	0
2	90	0	10
3	80	0	20
4	80	20	0
5	80	10	10
6	70	30	0
7	70	10	20
8	60	40	0
9	60	30	10
10	50	50	0
11	50	30	20
12	40	60	0
13	40	50	10
14	30	50	20

The received wood flour was pretreated with a NaOH solution before preparing the natural fiber reinforced HDPE composites. It was immersed in 10% NaOH solution for 60 min., followed by washing several times with deionised water, and finally with a 0.25*M* CH_3COOH solution.[21] The washings were continuously tested with a red litmus paper until they were neutral. They were then filtered under vacuum with a sintered glass funnel and dried in an oven at 105°C for 24 h. The dried agglomerated WF was then ground with a mortar and pestle to a fine powder and sieved with a 150 μm pore size sieve. The sample ratios are shown in Table I. All the samples were prepared by a melt mixing process using a Brabender Plastograph 50 mL internal mixer at 160°C and 35 rpm for 15 min. For the blends, the dry components were physically premixed and then fed into the heated mixer, whereas for the composites the WF was added into the Brabender mixing chamber within a minute after adding the premixed HDPE/wax blends. The samples were then melt-pressed at 170°C for 10 min under 100 kPa pressure using a hydraulic melt-press to form 15 × 15 cm^2 square sheets. Test samples were then cut from the sheets for various analyses.

Scanning electron microscopy (SEM) analyses were carried out using a Shimadzu ZU SSX-550 Superscan scanning electron microscope. Samples were frozen in liquid nitrogen, fractured by simply

breaking the specimen into an appropriate size to fit the specimen chamber, and then mounted onto the holder. Conductive coatings onto the sample surfaces were added using gold by a sputtering method before recording the SEM micrographs. Differential scanning calorimetry (DSC) analyses were done in a PerkinElmer Pyris-1 differential scanning calorimeter. The samples were run under nitrogen flow (flow rate 20 mL min^{-1}). The instrument was calibrated using the onset temperatures of melting of indium and zinc standards, as well as the melting enthalpy of indium. Samples (mass range 5–10 mg) were sealed in aluminum pans. The samples were heated from −40 to 160°C at a heating rate of 10°C min^{-1}, and cooled at the same rate. For the second scan, the samples were heated and cooled under the same conditions. The peak temperatures of melting and crystallization, as well as melting and crystallization enthalpies, were determined from the second scans to eliminate any thermal history effects. All the DSC measurements were repeated three times on different samples for each composition. The melting and crystallization temperatures, as well as enthalpies, are reported as average values with standard deviations. The TGA analyses were carried out on a PerkinElmer TGA7 thermogravimetric analyser. The samples (mass range 5–10 mg) were heated from 30 to 650°C at a heating rate of 20°C min^{-1} under flowing nitrogen (flow rate 20 mL min^{-1}). The dynamic mechanical properties of the blends and composites were investigated using a PerkinElmer Diamond DMA. The settings for the analyses were as follows:

Frequency 1 Hz
Amplitude 20 μm
Temperature range −140 to +100°C
Temperature program mode Ramp
Measurement mode Bending (dual cantilever)
Heating rate 5°C min^{-1}
Preloading force 0.02 N
Sample length 20 mm
Sample width 12.0–12.5 mm
Sample thickness 1.0–1.3 mm

A Hounsfield H5KS universal testing machine was used for tensile analysis of the samples. Dumbbell shaped samples of 75 × 13 mm, gauge length of 24 mm and neck width of 5 mm were tested at a speed of 50 mm min^{-1} under a load-cell force of 250.0 N. About five test specimens for each sample were analyzed, and the averages and standard deviations of the different tensile properties reported. For the determination of water absorption, test samples were initially weighed while dry, and then placed in deionized water at room temperature. The samples' water absorption was monitored for about 4 days at 10 and 14 h intervals. At every interval the samples were removed from the water, the surfaces dried with a water absorbent paper towel and weighed, and then replaced in the water. The percentage water absorption was calculated using eq. 1.

$$\%W_a = \frac{W_f - W_i}{W_i} \times 100 \quad (1)$$

where W_a is the total water absorbed, W_f is the final weight of the sample after a certain time t of water immersion, and W_i is the initial sample mass.

RESULTS AND DISCUSSION

Figure 1 shows the SEM micrographs of the 80/20 w/w HDPE/WF composite. The images show no visible WF fractures. The crystalline structure of the HDPE matrix is clearly visible in the areas around the WF particles. The WF particles seem clustered [A in Fig. 1(a)] within the polyethylene matrix, indicating poor filler dispersion. There are gaps [B in Fig. 1(a)] between the WF particles and the HDPE matrix, as well as some fiber pull-outs creating holes with smooth walls in the polymer matrix [C in Fig. 1(a)]. There is, however, evidence of some intimate contact between WF and HDPE, probably as a consequence of the alkali treatment of the WF that resulted into a rough surface allowing the polymer to adhere onto it through mechanical interlocking.[23,24] Aziz and Ansell[30] reported on the surface topography of untreated and alkalized fibers. They found that the treatment of hemp and kenaf with 6% NaOH removed the wax, oil and impurities and roughened the surface of the fiber bundles. Although there may be improved interaction between the WF and HDPE due to the WF pretreatment with an alkali, there was clearly still a poor interfacial adhesion between the HDPE matrix and the WF. This is in agreement with other published work on natural fiber reinforced HDPE composites.[25–29]

Figure 1(b–d) presents the micrographs of HDPE/20% WF (alkali treated) without wax and with various contents of M3 wax. It seems as if the M3 wax crystallized separately from the HDPE matrix. This separate crystallization behavior of M3 wax may be the result of its low molecular weight, and therefore lower viscosity. Therefore it is easy for the M3 wax to separate from the blends.[2] Figure 1(b) clearly shows a much more intimate contact between WF and the matrix, although it seems as if the WF is primarily covered by the wax. As the wax content increases, it becomes more difficult to observe individual WF particles, and to distinguish between the HDPE and wax phases [Fig. 1(c–d)]. This is probably the consequence of the higher affinity between WF and the wax, as well as the wax crystallizing separately in the amorphous phase of the HDPE. The

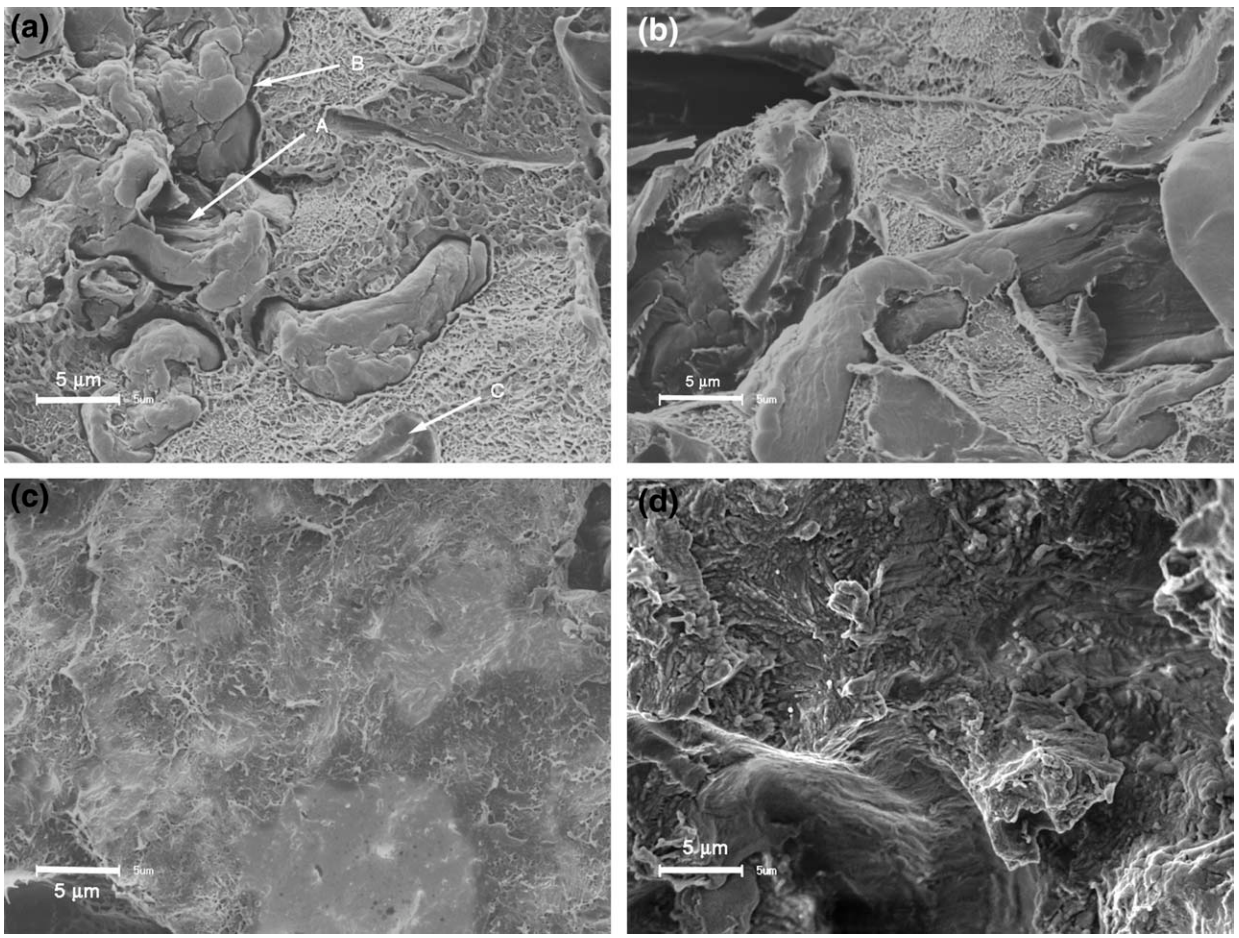

Figure 1 SEM micrographs of (a) 80/20 w/w HDPE/WF (alkali-treated), (b) 70/20/10 w/w HDPE/WF/M3 wax, (c) 50/20/30 w/w HDPE/WF/M3, and (d) 30/20/50 w/w HDPE/WF/M3 wax composites.

WF is most likely to be situated in this amorphous phase. Prior to the alkali treatment, the WF was covered by its natural wax and other components as described by Aziz and Ansell,[30] which were removed in the treatment process. Therefore it seems favorable for M3 wax to be attracted to the rough WF surfaces, also because of its shorter chains that will more easily penetrate the pores left after the alkali treatment of the WF.

The DSC heating results of the HDPE and the M3 wax are shown in Figure 2. The HDPE has a peak maximum at 136°C with an enthalpy of 158 J g^{-1}, whereas the M3 wax has a double peak at 33°C (peak shoulder) and 59°C (peak maximum). Its observed melting enthalpy is 150 J g^{-1}, which is lower than that of HDPE. The two endothermic peaks may be referred to as a solid–solid transition (at the peak shoulder) and melting.[1,2] In the case of HDPE/M3 wax blends, there are two separate endothermic peaks that are related to the melting peaks of the M3 wax and the HDPE. This behavior indicates that the HDPE is immiscible with the M3 wax at all the investigated compositions. This was also observed in our SEM results, where the M3 wax was observed to crystallize separately from the HDPE. The melting peak temperatures of the blends are shown in Table II. The melting temperatures of M3

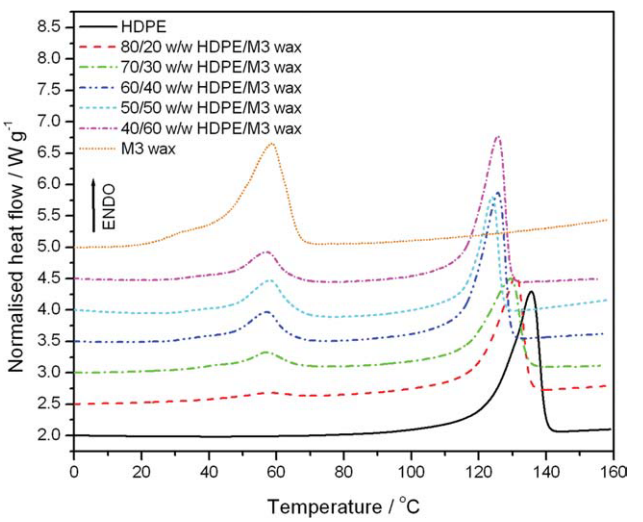

Figure 2 DSC heating curves of HDPE, M3 wax, and HDPE/M3 wax blends. [Color figure can be viewed in the online issue, which is available at www.interscience.wiley.com.]

TABLE II
Summary of DSC Results for HDPE/M3 Wax Blends and HDPE/WF/M3 Wax Composites

Samples	$T_{p,m} \pm sT_{p,m}$ (°C)	$\Delta H_m^{obs} \pm s\Delta H_m^{obs}$ (Jg^{-1})	ΔH_m^{calc} (Jg^{-1})
HDPE	135.9 ± 2.6	157.6 ± 13.2	–
M3 wax	58.8[a] ± 1.9	149.5 ± 4.1	–
	33.0[b] ± 1.0		
HDPE/M3 wax (w/w)			
80/20	55.9[c] ± 1.9	6.4 ± 1.6	29.9
	131.4[d] ± 2.0	102.2 ± 1.1	126.1
70/30	57.7[c] ± 0.8	13.6 ± 5.3	44.9
	130.4[d] ± 0.9	86.9 ± 2.5	110.3
60/40	57.3[c] ± 1.5	23.4 ± 1.2	59.8
	126.0[d] ± 1.5	93.3 ± 11.9	94.6
50/50	56.8[c] ± 1.3	32.7 ± 21.8	74.8
	124.7[d] ± 1.8	89.9 ± 15.4	78.8
40/60	56.9[c] ± 1.8	32.2 ± 23.1	89.7
	125.1[d] ± 2.5	82.8 ± 32.5	63.0
HDPE/WF/M3 wax (w/w)			
80/10/10	55.5[c] ± 0.6	1.5 ± 0.1	15.0
	132.9[d] ± 0.6	135.6 ± 3.0	126.1
60/10/30	56.9[c] ± 0.1	20.7 ± 1.8	44.9
	127.9[d] ± 0.7	105.2 ± 7.8	94.6
40/10/50	57.9[c] ± 0.3	55.6 ± 4.1	74.8
	123.4[d] ± 0.4	75.6 ± 2.6	63.0
70/20/10	55.2[c] ± 0.5	1.9 ± 0.3	15.0
	132.6[d] ± 0.9	121.4 ± 5.3	110.3
50/20/30	58.7[c] ± 1.4	23.5 ± 2.2	44.9
	129.0[d] ± 2.3	85.2 ± 3.4	78.8
30/20/50	58.7[c] ± 0.1	58.5 ± 4.7	74.8
	122.4[d] ± 0.3	53.8 ± 2.7	47.3

$T_{p,m}$, ΔH_m^{obs}, ΔH_m^{calc}, and s are respectively the peak temperature of melting, observed melting enthalpy, calculated melting enthalpy, and standard deviation,a and b indicate the first (maxima) and second (shoulder) peaks in the wax melting curve, and c and d indicate the wax and HDPE melting peaks in the blends/composites, respectively

wax remained fairly constant within experimental error with increasing wax content. However, an increase in wax content resulted in a decrease in the melting peak temperatures of HDPE. This is probably the result of the plasticization effect of the M3 wax on the HDPE matrix. This behavior was also reported by Krupa et al.[1] in their studies of PP/paraffin wax shape-stabilized phase change materials.

The experimentally observed melting enthalpies of the M3 wax are lower than the calculated enthalpies (Table II) for all the investigated wax contents. The calculated enthalpies were determined from the melting enthalpy of the unblended wax and the fractions of wax in the HDPE/M3 wax blends. The difference between the two enthalpies increases with an increase in wax content. Both these observations indicate that some portion of the M3 wax partially cocrystallized with HDPE. The standard deviations are large at high wax contents. This shows the inhomogeneity of the PCM blends and uneven wax dispersion within the polymer matrix at higher wax contents. In the case of HDPE melting, the experimentally observed melting enthalpies are lower than the calculated enthalpies at low wax contents. This may be due to the M3 wax plasticizing the HDPE matrix. However, the observed enthalpies are higher than the calculated enthalpies at higher wax contents, but the calculated enthalpies still fall within the error bars for the observed enthalpies. This supports the partial cocrystallization of the M3 wax with the HDPE at higher wax contents. The standard deviations for the observed melting enthalpies are also large at higher wax contents, which support the conclusion on the uneven distribution of the wax in the HDPE matrix.

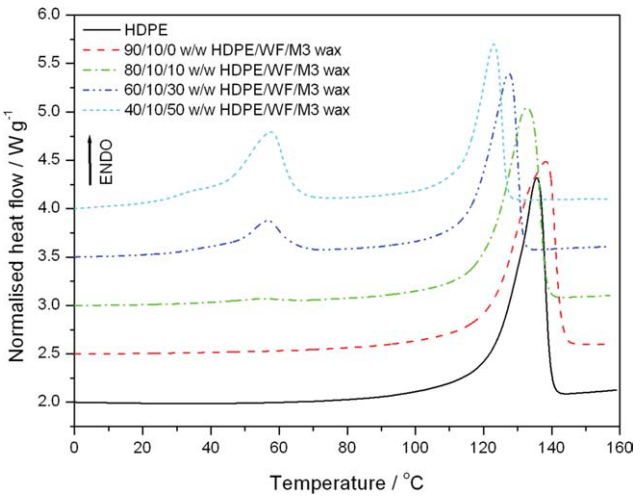

Figure 3 DSC heating curves of HDPE/WF/M3 wax PCM composites at 10% WF content. [Color figure can be viewed in the online issue, which is available at www.interscience.wiley.com.]

Figures 3 and 4 show the DSC heating curves of the HDPE/WF/M3 wax composites. The two figures

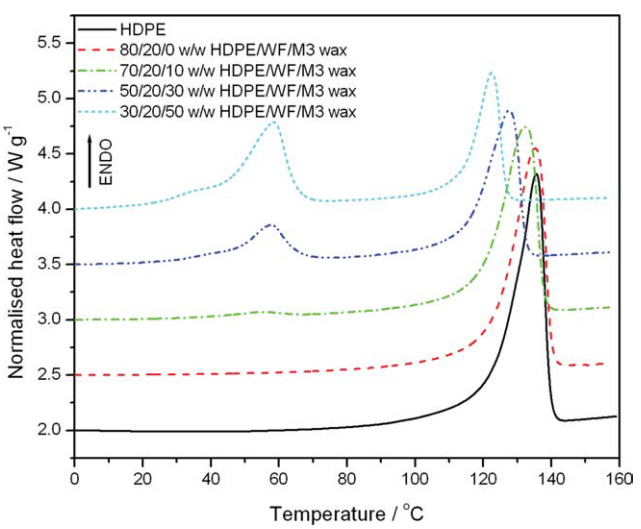

Figure 4 DSC heating curves of HDPE/WF/M3 wax PCM composites at 20% WF content. [Color figure can be viewed in the online issue, which is available at www.interscience.wiley.com.]

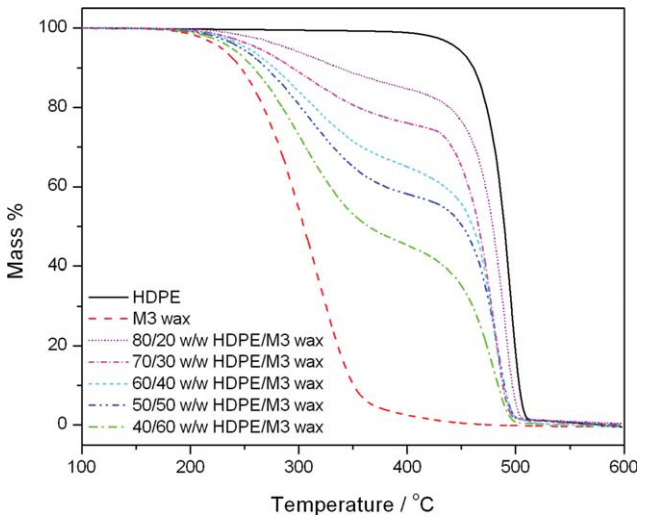

Figure 5 TGA curves of the HDPE/M3 wax blends. [Color figure can be viewed in the online issue, which is available at www.interscience.wiley.com.]

show similar behavior of two separate endothermic peaks (as in the case of the HDPE/M3 wax blends) for all the investigated M3 wax contents. This is a consequence of the high level of immiscibility of HDPE and M3 wax, also in the presence of WF. At low wax contents the melting temperatures of the wax are lower than that of pure wax, and the melting temperatures for the wax increased, whereas those of HDPE decreased with increasing wax content (Table II). The lower wax melting temperatures at low wax contents are attributed to a lower wax crystallinity because most of the wax penetrated the WF pores, which increased the amorphous fraction of the wax. At higher wax contents the WF pores were saturated with wax and the remaining wax crystallized around the WF particles. This increased the wax crystallinity and therefore the wax melting temperature. The decrease in HDPE melting temperature with increasing wax content is probably the result of the plasticizing effect of the molten wax in the polymer matrix.

For the melting enthalpies of M3 wax at 10 and 20% WF contents (Table II) it can be seen that the experimentally observed enthalpies are lower than the calculated enthalpies, and that the differences between them did not change significantly. This may be explained in terms of the following four situations: (i) as HDPE crystallizes first, there may be some inhibition of wax crystallization because of the isolation of single wax chains inside the amorphous phase of HDPE; (ii) part of the wax that was in contact with HDPE in the melt, may have cocrystallized with HDPE; (iii) part of the wax may have penetrated the pores of the WF particles, increasing the 'amorphous' part of the wax; (iv) part of the wax may have been adsorbed onto the surfaces of the WF particles, also increasing the 'amorphous' part of the wax. The standard deviations were fairly small, indicating that samples were more homogeneous. The experimentally observed melting enthalpies of the HDPE in the HDPE/WF/M3 wax composites are higher than the calculated enthalpies with almost constant differences. This is probably the result of the partial cocrystallization of some of the M3 wax with the HDPE in the presence of WF. The standard deviations are small, indicating that the samples were fairly homogeneous.

The TGA results show that the HDPE and M3 wax decomposed completely in a single step, whereas WF decomposed in multiple steps and yielded some residue (Figs. 5 and 6). The HDPE matrix has the highest thermal stability, followed by the WF, and then the M3 wax. The TGA curve of the alkali-treated and dried WF shows an initial weight loss step (5–6%) around 100°C (Figs. 6 and 7). This is a consequence of moisture evaporating from the sample, which probably readsorbed almost immediately after drying. This weight loss step is not visible in the composites, because the loosely bound water probably evaporated very quickly from the fiber surfaces during the mixing at 160°C. The second, major decomposition step in the range of 250 to 360°C is the result of the thermal depolymerization of hemicelluloce and the glycosidic linkages of cellulose. The final decomposition step, starting above 360°C, may be the result of lignin decomposition, which finally contributes to the formation of char above 450°C.[31,32]

The blends degraded in two steps, with the M3 wax destabilizing the HDPE (Fig. 5). Both degradation steps correspond with the relative amount of each component in the blends according to the

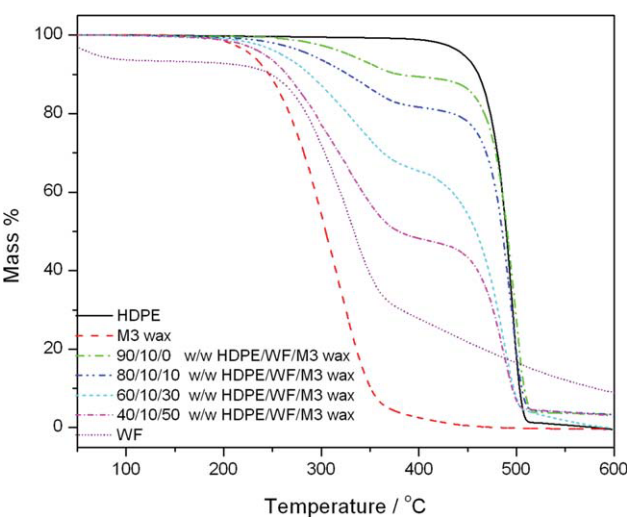

Figure 6 TGA curves of HDPE/10% WF/M3 wax composites. [Color figure can be viewed in the online issue, which is available at www.interscience.wiley.com.]

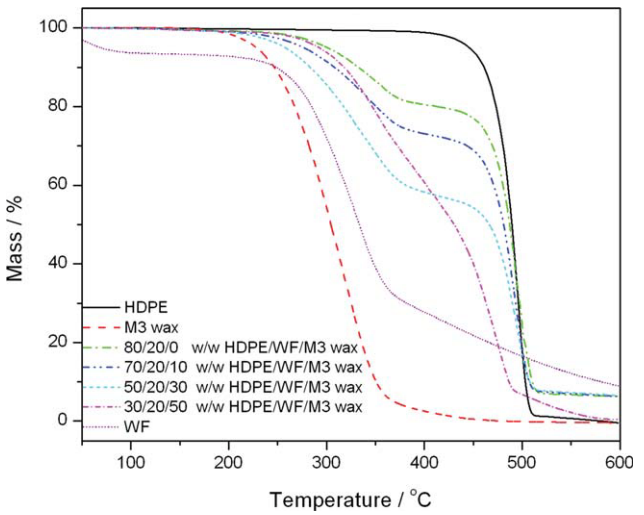

Figure 7 TGA curves of HDPE/20% WF/M3 wax composites. [Color figure can be viewed in the online issue, which is available at www.interscience.wiley.com.]

sample compositions. Therefore the first step is related to the degradation of M3 wax and the second to that of the HDPE matrix. This may be attributed to the immiscibility of the HDPE and the M3 paraffin wax, as already seen from both the DSC and SEM results. Krupa et al.[1,2] reported similar behavior for soft wax (Wax S) blended with PP and LDPE matrices. The thermal stabilities of the blends fall between those of the wax and the HDPE. This is probably because of both the low molecular weight and low thermal stability of the paraffin wax. The increased concentration of short wax chains, as well as fragments formed by chain scission, will have enough energy to escape from the matrix at lower temperatures. The free radicals formed during wax degradation will also initiate HDPE degradation at lower temperatures.

Figures 6 and 7 presents the TGA results of the HDPE/WF/M3 wax composites. All the PCM composites degraded in two steps. The percentage degradation during the first step corresponds to a combination of the amounts of WF and M3 wax initially mixed into the sample, and the second to the initial content of HDPE. The first degradation step is an overlapping of the decompositions of the WF and M3 wax, with the M3 wax degrading first. For both WF contents, the presence of wax reduced the thermal stability of the composites, but not more than that observed for the HDPE/M3 wax blends.

The DMA storage and loss modulus of the HDPE/M3 paraffin wax blends are shown as a function of temperature in Figure 8. HDPE has the highest storage modulus over the whole investigated temperature range. Depending on temperature interval, two opposite trends are noticed with increasing wax content. From −150 to −42°C, samples with the highest wax content show a higher modulus, whereas from −42 to 60°C the storage modulus decreases with increasing wax content. It is not clear why there is an increase in storage modulus around 50°C for the blends, but it may be related to the solid–solid transition that the wax undergoes in this temperature region (see discussion of DSC results). The loss modulus curve of neat HDPE in Figure 9 shows two transition peaks. The first peak at −125°C corresponds to the γ-transition and is the result of the crankshaft relaxation mechanism of the PE chains.[33] The second peak, at 46°C, is the α-relaxation transition and it is related to the crystalline fraction in the semicrystalline material. There is virtually no change in the γ-transition peak position with the addition of wax, but the position of the α-relaxation shifts to lower temperatures. Although the reduced melting temperature of HDPE in the presence of wax has been related to the plasticization effect of the wax, it may also have been the

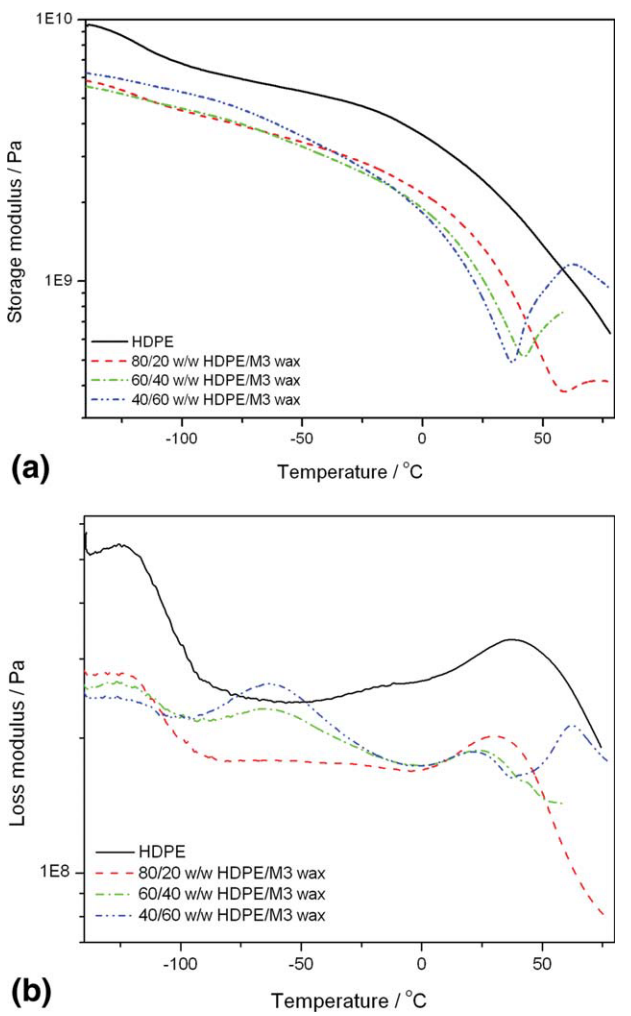

Figure 8 DMA (a) storage modulus and (b) loss modulus curves for the HDPE/M3 wax blends. [Color figure can be viewed in the online issue, which is available at www.interscience.wiley.com.]

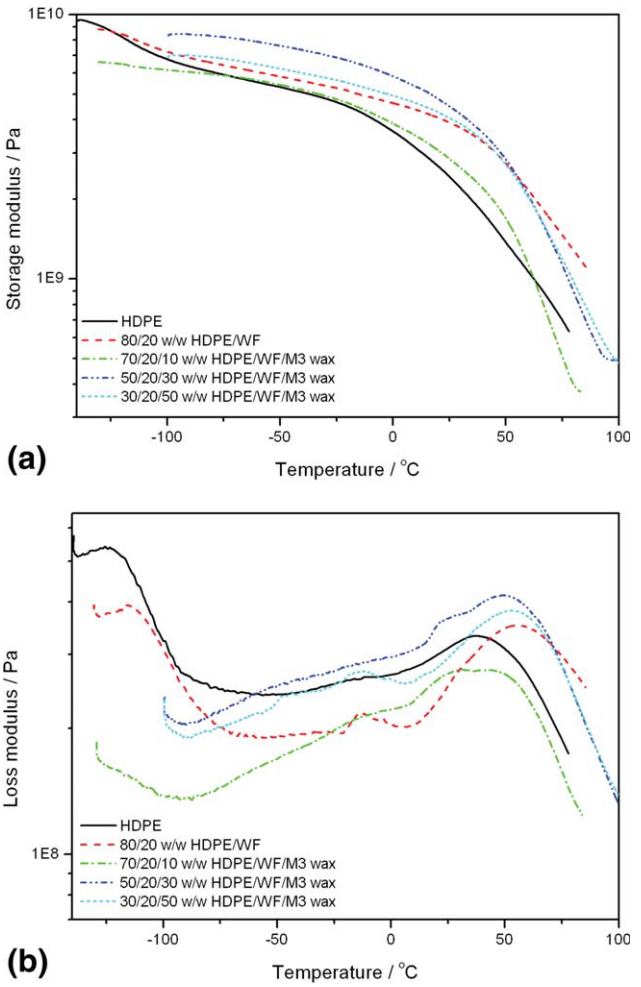

Figure 9 DMA (a) storage modulus and (b) loss modulus curves for the HDPE/WF/M3 wax composites. [Color figure can be viewed in the online issue, which is available at www.interscience.wiley.com.]

result of a reduction in lamellar thickness. The lower α-relaxation temperature may then have been the result of the thinner lamellae. Sirotkin and Brooks[34] reported the association of the α-relaxation with c-shear within the crystalline lamellae, and concluded that this transition is dependent only on the lamellar thickness. The loss modulus curves of the samples with 40 and 60% M3 wax [Fig. 8(b)] show an additional peak at −75°C, which is the β-relaxation. Linear polyethylenes (LPE) usually do not show a β-relaxation, which normally occurs in branched polyethylenes (BPE). This transition is the result of the motion in the interfacial regions (amorphous portion between crystallites) of the semicrystalline material, and depends on the degree of branching.[34,35] Djoković et al.[35] reported that the minimal interfacial content, which can produce a visible β-peak in the DMA curve of polyethylene, is about 10% of semicrystalline material. In LPE the interfacial content is about 3–4%, whereas in BPE (with only 0.6 mol % branches) it is about 11%. Long branches affect this relaxation more than shorter ones. The presence of a β-relaxation in the HDPE/M3 wax blends is therefore probably the result of an increase in the amount of the interfacial amorphous content as the wax content increases.

Figure 9 shows the storage and loss modulus for the HDPE/WF/M3 wax composites. No specific trends related to the presence of WF or wax content are observable in the storage modulus plots [Fig. 9(a)]. The addition of the WF to neat HDPE lowered the loss modulus [Fig. 9(b)], and it induced a shift of both the γ- and α- transitions towards high temperatures. This is attributed to a restriction of the motion of the polymer chains, as well as increased lamellar thickness with WF loading. An additional peak at −14°C is noticed after WF incorporation. We could not find an explanation for the origin of this transition, but this transition seems to be dependent on the wax content. Also, as in the case of the HDPE/M3 wax blends (Fig. 8), the position of the α-relaxation transition shifts to lower temperatures as wax content increases, but it still appears at a higher temperature than that of the neat HDPE.

The stress–strain curves of HDPE show that it exhibited the typical characteristics of ductile polymers: stress whitening followed by necking and cold drawing after yielding. It has the highest values of elongation at break (588%) and modulus (653 MPa). When 20 wt % M3 wax is introduced, the blend shows strain softening after yielding. An increase in elongation at yield and a slight decrease in yield stress (Table III, 80/20 w/w HDPE/M3 wax sample) can be noticed. This increase in elongation at yield may be the result of the plasticization effect of the M3 wax on the HDPE matrix, whereas the decrease in yield stress is because of the lower crystallinity of the blends as the wax content increases. Samples with high wax contents did not show any yield point, and they were very brittle.

Table III shows the Young's modulus of the HDPE/M3 wax blends as function of wax content. A decrease in modulus with an increase in M3 wax content can be seen. This is a consequence of the decreased crystallinity of the blends with wax increase as seen by DSC. The tensile strength varies with wax loading, and the elongation at break of the blends decreases with increasing wax content (Table III). The lowered tensile strength may be the result of the decreased crystallinity of the blends with increasing wax content, and the shorter wax chains that may have partially cocrystallized with the HDPE, decreasing the average number of tie-chains between the HDPE lamellae. This led to a suppression of the cold drawing deformation of the polymer matrix. The effect on the elongation at break is a consequence of the loss of drawability in the

TABLE III
Summary of Tensile Results for HDPE/M3 Wax Blends and HDPE/WF/M3 Wax Composites

Sample w/w	$\varepsilon_y \pm s\varepsilon_y$ (%)	$\sigma_y \pm s\sigma_y$ (MPa)	$\varepsilon_b \pm s\varepsilon_b$ (%)	$\sigma_b \pm s\sigma_b$ (MPa)	$E \pm s$E (MPa)
HDPE	11.3 ± 0.5	29.2 ± 1.1	588 ± 29	18.8 ± 0.8	653 ± 31
HDPE/M3 wax					
80/20	14.8 ± 0.2	28.6 ± 0.7	270 ± 9	15.3 ± 1.0	620 ± 6
70/30	–	–	14.1 ± 0.4	23.1 ± 0.3	559 ± 45
60/40	–	–	14.1 ± 1.3	21.0 ± 0.4	511 ± 4
50/50	–	–	10.7 ± 0.5	17.2 ± 0.3	456 ± 17
40/60	–	–	12.8 ± 0.3	16.7 ± 1.3	404 ± 11
HDPE/WF/M3 wax					
80/10/10	–	–	10.9 ± 0.9	23.9 ± 0.8	838 ± 31
60/10/30	–	–	8.6 ± 0.7	22.3 ± 0.7	610 ± 12
70/20/10	–	–	5.4 ± 0.5	19.8 ± 1.2	807 ± 48

ε_y, σ_y, ε_b, σ_b, and E are elongation at yield, yield stress, elongation at break, stress at break, and Young's modulus of elasticity, respectively, and $s\varepsilon_y$, $s\sigma_y$, $s\varepsilon_b$, $s\sigma_b$, and sE are their respective standard deviations.

presence of high wax contents that leads to highly brittle blend samples.

Young's modulus of the HDPE/WF/M3 wax composites decreases with increasing wax content at 10 wt % WF content. This is because of reduced contact/interaction between the WF and the HDPE matrix in the presence of wax. As seen by SEM, the wax covered the WF particles and thus prohibited the mechanical interlocking interaction between WF and HDPE. As a result the wax has a considerable influence on the mechanical properties of the composites by reducing their stiffness. It may also be a consequence of the lower crystallinity of these composites as seen by DSC. Only samples with up to 30 wt % M3 wax content could be subjected to tensile tests because of the highly brittle samples at higher wax contents. However, there was an increase in Young's modulus with the introduction of 10 wt % wax to composites containing 20% WF. This may probably be the result of too little wax available to cover all of the WF particles, and therefore some WF particles were directly in contact with the polymer matrix. Only the 10 wt % M3 wax composite could be characterized under tensile as the rest of the samples were also highly brittle.

The stress at break of the HDPE/WF (10%)/M3 wax composites decreased with increasing wax content (Table III). As the tensile strength is a function of crystallinity, this is to be expected because of the decreased crystallinity as seen by DSC. It may also be the result of the poor interaction between WF and HDPE, even in the presence of wax. In the case of the HDPE/WF (20%)/M3 wax composites, an increase in stress at break with increasing wax content is seen. As there is more WF than wax in this system, it is probably the result of some interaction between the WF and the HDPE matrix. The elongation at break of the HDPE/WF (10%)/M3 wax decreased with an increase in wax content. This is a consequence of the restricted mobility of the polymer chains and reduced strain transfer in the presence of both WF and wax, which resulted into highly brittle composite samples. For the 20% WF composites, there is a slight increase in elongation at break. This may be the result of the plasticization effect of the M3 wax.

Figures 10 and 11 show the water absorption curves of the HDPE/WF/M3 wax composites, at 10 and 20 wt % WF. A decrease in water uptake is seen with increasing wax content. This is the result of the presence of wax that is water repellent in nature. As seen by SEM and DSC, the wax covers the WF surfaces in these composites and therefore limits the exposure of wood flour particles to water. At 10 wt % WF content, the differences between the water uptake of the composites at various wax contents is small, whereas at 20% it is significantly larger. This

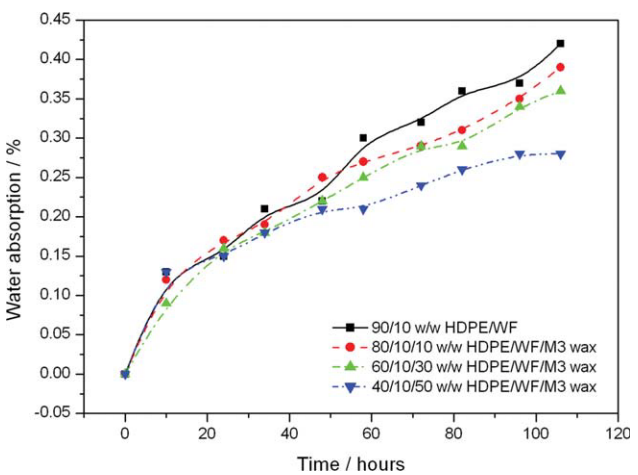

Figure 10 Water absorption curves of HDPE/WF/M3 wax composites at 10 wt % WF and various wax contents. [Color figure can be viewed in the online issue, which is available at www.interscience.wiley.com.]

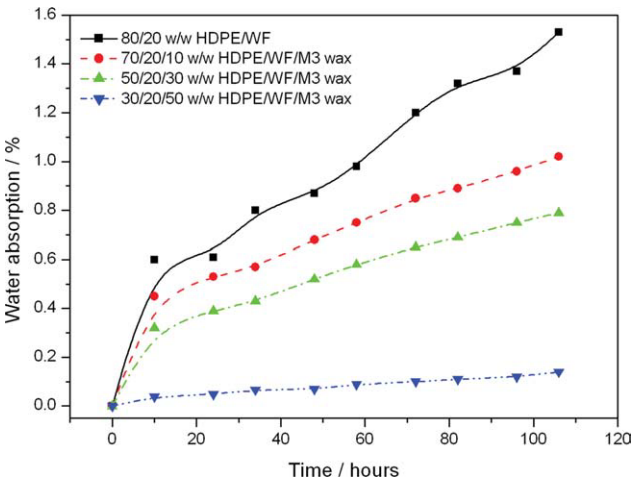

Figure 11 Water absorption curves of HDPE/WF/M3 wax composites at 20 wt % WF and various wax contents. [Color figure can be viewed in the online issue, which is available at www.interscience.wiley.com.]

is because at low WF content (10%) almost all the WF particles are effectively covered by small amounts of wax. At high content of WF (20%), the low amounts of wax did not effectively cover all the WF particles, which remained exposed to water. However, as the wax content increased, most of the filler particles were effectively covered by wax, which has also filled the pores and limited water uptake by the composites.

CONCLUSIONS

The structure and properties of phase change materials based on high density polyethylene, a soft Fischer-Tropsch paraffin wax and alkali-treated wood flour were investigated. The composites showed some evidence of intimate contact between the WF and the HDPE matrix as a result of alkali treatment, but poor filler dispersion and poor interfacial adhesion were still observed. The HDPE and wax were partially immiscible, and the WF was primarily covered by wax. The presence of the wax both reduced the crystallinity and plasticized the HDPE matrix. Partial cocrystallization of the wax and polymer, inhomogeneity and uneven wax dispersion within the polymer matrix were observed. The wax distribution in the HDPE/WF/wax composites was determined by the WF particle distribution, because the wax seemed to be concentrated around the WF particles. The presence of wax reduced the thermal stability of the HDPE/WF/wax composites, but not more than that observed for the HDPE/wax blends. Both the wax and the WF influenced the viscoelastic behavior of the HDPE matrix in the blends and composites. The presence of wax resulted in an increase in the amount of the interfacial amorphous content of the HDPE/wax blends. The mechanical properties of the blends were poor in the presence of wax, but improved with WF content in the composites. The water absorption by the composites decreased with an increase in wax content.

Effective energy storage requires the phase change material (in this case the wax) to be immiscible with the matrix material (in this case HDPE). Although the M3 wax has a lower melting enthalpy, its high level of immiscibility makes it suitable as an energy storage material when blended with HDPE. It seems that the presence of wood flour reduced cocrystallization of the wax with HDPE, because it seemed to interact more strongly with the wax so that the wax primarily crystallized around the WF particles. This resulted in a somewhat greater portion of the wax being available for energy storage. However, it was found that the presence of wood flour did not improve the tensile properties of the PCM blends, as was envisaged at the start of the project.

References

1. Krupa, I.; Miková, G.; Luyt, A. S. Eur Polym J 2007, 43, 895.
2. Krupa, I.; Miková, G.; Luyt, A. S. Eur Polym J 2007, 43, 4695.
3. Regin, A. F.; Solanki, S. C.; Saini, J. S. Renewable Sustainable Energy Rev 2008, 12, 2438.
4. Tyagi, V. V.; Buddhi, D. Renewable Sustainable Energy Rev 2007, 11, 1146.
5. Sharma, A.; Tyagi, V. V.; Chen, C. R.; Buddhi, D. Renewable Sustainable Energy Rev 2009, 13, 318.
6. Farid, M. M.; Khudhair, A. M.; Razack, S. A. K.; Al-Hallaj, S. Energy Conversion Manage 2004, 45, 1597.
7. Kenisarin, M.; Mahkamov, K. Presented at NATO Advanced Study Institute Summer School on Thermal Energy Storage for Sustainable Energy Consumption (TESSEC), Çeşme, Izmir, Turkey, June 6–17, 2005.
8. Akgün, M.; Aydin, O.; Kaygusuz, K. Energy Conversion Manage 2007, 48, 669.
9. Sari, A. Energy Conversion Manage 2004, 45, 2033.
10. Hasnain, S. M. Energy Conversion Manage 1998, 39, 1127.
11. Xiao, M.; Feng, B.; Gong, K. Energy Conversion Manage 2002, 43, 103.
12. Bader, M. Microencapsulated Paraffin in Polyethylene for Thermal Energy Storage; The University of Auckland: New Zealand, 2002.
13. Hato, M. J.; Luyt, A. S. J Appl Polym Sci 2007, 104, 2225.
14. Krupa, I.; Luyt, A. S. Polymer 2001, 42, 7285.
15. Krupa, I.; Luyt, A. S. Thermochim Acta 2001, 372, 137.
16. Inaba, H.; Tu, P. Heat Mass Transfer 1997, 32, 307.
17. Hong, Y.; Xin-Shi, G. Sol Energy Mater Sol Cells 2000, 64, 37.
18. Beginn, U. Macromol Mater Eng 2003, 288, 245.
19. Zhao, Y.; Wang, K.; Zhu, F.; Xue, P.; Jia, M. Polym Degrad Stab 2006, 91, 2874.
20. Bledzki, A. K.; Gassan, J. Prog Polym Sci 1999, 24, 221.
21. Joseph, P. V.; Joseph, K.; Thomas, S. Compos Sci Technol 1999, 59, 1625.
22. Kim, J.-P.; Yoon, T.-H.; Mun, S.-P.; Rhee, J.-M.; Lee, J.-S. Bioresour Technol 2006, 97, 494.
23. John, M. J.; Anandjiwala, R. D. Polym Compos 2008, 29, 187.
24. Cao, Y.; Shibata, S.; Fukumoto, I. Compos A 2006, 37, 423.

25. Bengtsson, M.; Gatenholm, P.; Oksman, K. Compos Sci Technol 2005, 65, 1468.
26. Lai, S.-M.; Yeh, F.-C.; Wang, Y.; Chan, H.-C.; Shen, H.-F. J Appl Polym Sci 2003, 87, 487.
27. Wang, Y.; Yeh, F.-C.; Lai, S.-M.; Chan, H.-C.; Shen, H.-F. Polym Eng Sci 2003, 43, 933.
28. Lu, J. Z.; Wu, Q.; Negulescu, I. I. J Appl Polym Sci 2005, 96, 93.
29. Lu, J. Z.; Negulescu, I. I.; Wu, Q. Compos Interface 2005, 12, 125.
30. Aziz, S. H.; Ansell, M. P. Compos Sci Technol 2004, 64, 1219.
31. Marcovich, N. E.; Villar, M. A. J Appl Polym Sci 2003, 90, 2775.
32. Albano, C.; González, J.; Ichazo, M.; Kaiser, D. Polym Degrad Stab 1999, 66, 179.
33. Heaton, N. J.; Benavente, R.; Pérez, E.; Bello, A.; Pereňa, M. Polymer 1996, 37, 3791.
34. Sirotkin, R. O.; Brooks, N. W. Polymer 2001, 42, 9801.
35. Djoković, V.; Kostoski, D.; Dramićanin, M. D. J Polym Sci Part B: Polym Phys 2000, 38, 3239.